



ARTICLE

# Halogen-Free Flame Retarded Poly(Lactic Acid) with an Isosorbide-Derived Polyphosphonate

Wenwen Guo<sup>1,2,3</sup>, Wei Cai<sup>3</sup>, Dong Wang<sup>1</sup>, Junling Wang<sup>4</sup>, Xiefei Zhu<sup>5,\*</sup> and Bin Fei<sup>2,\*</sup>

<sup>1</sup>Key Laboratory of Eco-Textiles, Ministry of Education, College of Textile Science and Engineering, Jiangnan University, Wuxi, 214122, China

<sup>2</sup>Institute of Textiles and Clothing, The Hong Kong Polytechnic University, Hung Hom, Hong Kong, China

<sup>3</sup>State Key Laboratory of Fire Science, University of Science and Technology of China, Hefei, 230026, China

<sup>4</sup>Jiangsu Key Laboratory of Hazardous Chemicals Safety and Control, College of Safety Science and Engineering, Nanjing Tech University, Nanjing, 211816, China

<sup>5</sup>Department of Thermal Science and Energy Engineering, University of Science and Technology of China, Hefei, 230026, China

\*Corresponding Authors: Bin Fei. Email: bin.fei@polyu.edu.hk; Xiefei Zhu. Email: xiefzhu@mail.ustc.edu.cn

Received: 19 August 2021 Accepted: 15 October 2021

## ABSTRACT

Fabrication of flame retardants from renewable biomass has aroused extensive interest over the past decade. This work reported a synthesis of isosorbide-derived polyphosphonate (PICPP) as an anti-flammable agent for poly(lactic acid) (PLA). The presence of PICPP notably declined the storage modulus of PLA/PICPP owing to the declined molecular weight of PLA catalyzed by the presence of PICPP. PLA and PLA/PICPP thermally degraded in one stage under either air or nitrogen atmosphere. With increasing the amount of PICPP, the onset thermal decomposition temperature of PLA/PICPP was decreased gradually, owing to the earlier decomposition of PICPP. With only 10 wt% of PICPP, PLA/PICPP-10 achieved a high limiting oxygen index of 30.0% and UL-94 V-0 classification, manifesting that PICPP was an efficient anti-flammable agent for PLA. The inclusion of 15 wt% PICPP also caused 33% and 16% decline in PHRR and THR of PLA, respectively. TG-IR results clarified that PLA/PICPP produced the less typical pyrolysis products especially flammable carbonyls than PLA, which may account for the suppressed PHRR and THR values of PLA/PICPP.

## KEYWORDS

Isosorbide; polyphosphonate; poly(lactic acid); flame retardancy

## 1 Introduction

Poly(lactic acid) (PLA) is one kind of thermoplastic biodegradable polymeric material, which is sourced from starch-rich plants such as cassava, corn, and so on. PLA has many advantages, including rich raw materials, biodegradability, excellent biocompatibility, superior processing and mechanical properties [1–3]. Given this, PLA has been extensively applied in biomedical, packaging materials and other related fields. However, similar to the conventional polyesters, PLA is easy to ignite in the air and accompanied by serious dripping phenomenon, which seriously restricts the application of PLA in the fields with high



flame-retardant requirements such as electronic packaging and automobile industry [4,5]. Hence, the attempt to enhance the anti-flammability of PLA has become the focus of both academia and industry.

At present, physical blending flame retardant modification is the most commonly used method for flame-retardant modification of PLA, which refers to the processing of flame retardant PLA materials by adding flame retardants to PLA matrix through melt blending. This strategy possessed the advantages of low cost, convenient operation and easy commercialization. The commonly used additive flame retardants is mainly divided into two categories which are organic and inorganic anti-flammable agents. The organic anti-flammable agents for PLA include phosphorus-based chemicals [6–8], phosphorus/nitrogen-based chemicals [9,10], intumescent flame-retardant systems [11–13], etc., among many organic flame retardants, the phosphorus-containing compounds have become the most popular flame-retardants for PLA owing to their merits of low smoke and environmental friendliness. So far, diverse phosphorus-based flame-retardant additives including 9, 10-dihydro-9-oxa-10-phosphaphenanthrene-10-oxide (DOPO)-derived chemicals [14–19], hypophosphorous acid-based derivatives [6], poly(ethylene diglycol phenylphosphinate) [20], poly(1, 2-propanediol 2-carboxyethyl phenyl phosphinate) [21], poly(butylene phenyl phosphate) [22], hyperbranched polyphosphate ester [23], and poly(phenylphosphoryl phenylenediamine) [24], have been synthesized for improving the anti-flammability of PLA. However, in order to achieve satisfactory flame retardant effect, it is necessary to add a high content (usually beyond 15%) of phosphorus-based flame-retardant additives to PLA.

Except for the organic flame-retardants, various inorganic flame-retardants such as carbon-based materials [25–28], metal organic frameworks [29,30], silicates [31–34], black phosphorus [35], graphitic carbon nitride [36], molybdenum disulfide [37,38], have been utilized to enhance the anti-flammability of PLA. Compared to organic flame-retardants, inorganic anti-flammable agents are more efficient in decreasing the heat release and smoke emission at a relatively low dosage. However, the use of inorganic flame-retardants alone generally makes PLA difficult to reach UL-94 V-0 classification. Thus, inorganic flame-retardants are mostly used together with organic flame-retardants to create a flame-retardant synergism.

Based on the review of the anti-flammable strategies above, highly efficient anti-flammable technology for PLA remains a challenging task. Recently, the application of bio-based flame retardants for PLA is becoming a new-arising trend [39–42]. As a sucrose-derived diol, isosorbide has attracted extensive attention because of its high stiffness and thermal stability [43]. Isosorbide has been reported to fabricate the flame-retardants for epoxy [44,45] and poly(butylene succinate) [46]. Recently, Wang and collaborators designed a isosorbide-derived poly(phosphoester) as flame-retardant for PLA [47]. PLA containing 20 wt% of isosorbide-derived poly(phosphoester) achieved a LOI of 25.5% and passed UL-94 V-0 classification. To develop isosorbide derivatives with higher flame-retardant efficacy, an isosorbide-derived polyphosphonate was produced via condensation between 2-carboxyethyl phenylphosphinic acid and isosorbide in this study. The effect of the isosorbide-derived polyphosphonate dosage on the thermal and flame-retardant behaviors was investigated. Finally, the flame-retardant mechanism of this isosorbide-derived polyphosphonate was speculated based on the analysis of the pyrolysis products of PLA composites.

## 2 Experimental Section

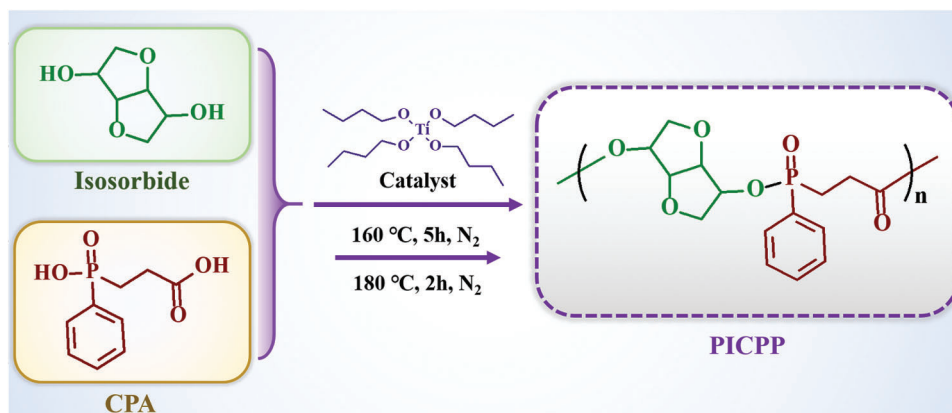
### 2.1 Materials

Poly(lactic acid) (2003D) were purchased from Nature Works (USA). Isosorbide and 2-carboxyethyl phenylphosphinic acid (CPA) were offered by Aladdin Bio-Chem Technology Co., Ltd., (China). Tetrabutyl titanate was obtained from Sinopharm Chemical Reagent Co., Ltd., (China).

### 2.2 Synthesis of Poly(Isosorbide 2-Carboxyethyl Phenyl Phosphinate) (PICPP)

The PICPP was synthesized through polycondensation of CPA and isosorbide (Scheme 1). Briefly, CPA (0.50 mol, 107.1 g), isosorbide (0.55 mol, 80.4 g) and tetrabutyl titanate (0.6 g, as the catalyst) were introduced

into a three-necked flask fitted with a condenser, a mechanical stirrer as well as a nitrogen inlet. The reaction was conducted at 160°C for 5 h under N<sub>2</sub>. Afterwards, the temperature was then raised to 180°C for 2 h. Subsequently, a vacuum (<100 Pa) was applied and maintained for 5 h to complete the polycondensation process. At last, the light-yellow product was obtained and ground into powder at room temperature.



**Scheme 1:** Polycondensation of between isosorbide and 2-carboxyethyl phenylphosphinic acid to yield bio-based polyphosphinate

### 2.3 Fabrication of PICPP/PLA Blends

All the PICPP/PLA composites were prepared using a torque rheometer (XSS300, Kechuang, China) at 170°C for 10 min. Various contents of PICPP ranging from 5 to 15 wt% were incorporated into PLA resin. After melt compounding, the PICPP/PLA mixture was ground into pellets and then injected to a micro-injection machine (WZS10-D, China) for preparation of specimens of LOI, UL-94 and tensile tests. The cylinder temperature was 180°C and the molding temperature was set to 50°C.

### 2.4 Methods

Fourier-transform infrared (FTIR) spectroscopic analysis was carried out on a Nicolet iS50 spectrophotometer using potassium bromide disc approach.

Proton and <sup>31</sup>P-nuclear magnetic resonance (NMR) spectroscopic analysis was performed on an AVANCE III 400 MHz instrument using deuterated chloroform as solvent.

Molecular weight and molecular weight distribution of the samples were determined by a Dionex Ultimate 3000 gel permeation chromatography (GPC). The temperature of DMF eluent was 35°C and the flow rate was 0.5 mL/min.

Dynamic mechanical analysis (DMA) was carried out with a TA Q850 analyzer at a ramp rate of 5 °C/min. The specimen used was of 35 mm × 10 mm × 3 mm.

Thermogravimetric analysis (TGA) was performed on a TA Q500 apparatus. The ramp rate was 20 °C/min from 30 to 800°C.

Anti-flammable behaviors were assessed by an HC-2 limiting oxygen index (LOI) apparatus (Sample size: 100 mm × 6.5 mm × 3 mm) and a CFZ-2 vertical burning chamber (Sample size: 130 mm × 13 mm × 3 mm).

Heat-related parameters were obtained using an FTT microscale combustion calorimeter (MCC). The sample was thermally decomposed from 100 to 650°C at a ramp rate of 1°C/s under N<sub>2</sub> (flow rate: 80 mL/min). The pyrolysis volatiles were then blended with a 20 mL/min stream of O<sub>2</sub>. The mixture was finally sent to a 900°C combustor. On the basis of the oxygen consumption principle, the heat release rate was computed.

Pyrolysis products during TGA measurements were detected by a Nicolet 6700 FTIR spectrophotometer whose gas chamber was linked to a TA Q50 thermal analyzer through a stainless tube (TGA-FTIR).

### 3 Results and Discussion

The chemical structure of PICPP was characterized using the FTIR instrument. As shown in Fig. 1, CPA exhibits an intense band centered at the 3419 cm<sup>-1</sup> that is ascribed to the -OH groups of carboxylic and phosphorus acid, and the absorption peaks at 2925 and 2872 cm<sup>-1</sup> are assigned to the asymmetric and symmetric stretching vibration of -CH<sub>2</sub>- groups, respectively. The absorption peaks of isosorbide at 2937 and 2875 cm<sup>-1</sup> are related to the symmetric and asymmetric stretching vibration of -CH<sub>2</sub>- groups, respectively. The broad absorption peak at 3397 cm<sup>-1</sup> is assigned to the -OH group, and the absorption peak at 1077 cm<sup>-1</sup> originated from the C-O-C group in the pentacyclic structure. Compared to the monomers, the stretching vibration of the hydroxyl groups almost disappears in PICPP attributed to the occurrence of esterification between CPA and isosorbide. Additionally, the absorption band appearing at 1221 cm<sup>-1</sup> belongs to the formation of C-O-C<sub>isosorbide</sub>.

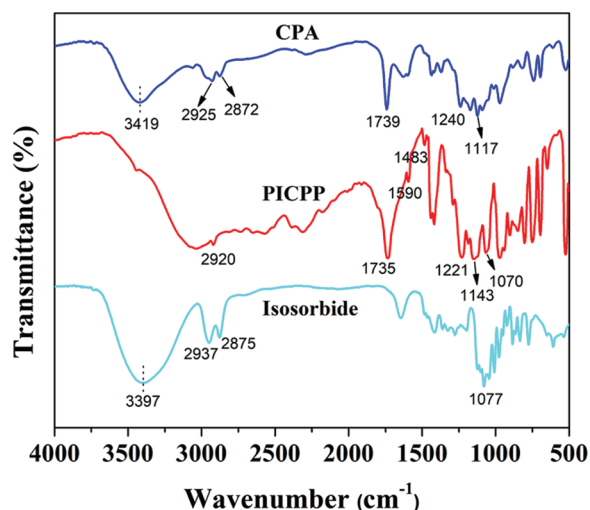


**Figure 1:** FTIR spectral analysis of CPA, isosorbide and PICPP

Fig. 2 depicts the proton and <sup>31</sup>P-NMR spectra of PICPP. As shown in Fig. 2a, the multiple signals at the chemical shift range from 3.5 to 5.2 ppm (marked 1–6) are ascribed to the protons belonging to the isosorbide cycle. The multiple signals ranging from 7.4 to 7.8 ppm are allocated to the aromatic protons. Additionally, the signals at 2.6 and 2.2 ppm are assigned to the protons in the -CH<sub>2</sub>-P(O)- (marked 7) and -CH<sub>2</sub>-C(O)- (marked 8) groups, respectively. An intense signal at 43.1 ppm is observed in the <sup>31</sup>P-NMR spectrum of PICPP (Fig. 2b), implying only one chemical environment for phosphorus atoms. These data correspond well with the anticipated molecular structure, manifesting the successful synthesis of PICPP.

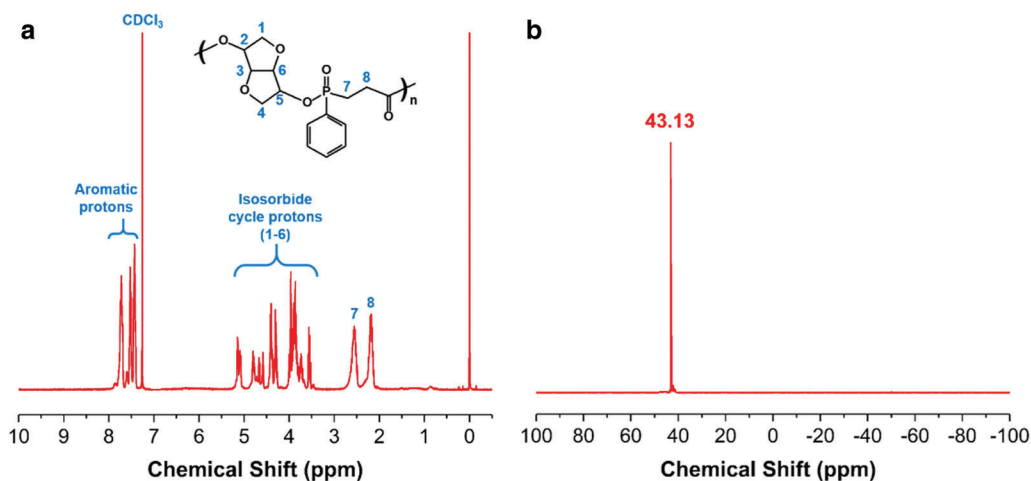


**Figure 2:** (a) Proton and (b)  $^{31}\text{P}$ -NMR spectra of PICPP

Polymers' molecular weight is a key factor to affect their performances. The influence of PICPP on the molecular weight of PLA composites was characterized using GPC. Table 1 lists the GPC data of PLA and PLA/PICPP. With the increase of the addition content of PICPP, both the number-average molecular weight ( $M_n$ ) and weight-average molecular weight ( $M_w$ ) were declined gradually. Polydispersity index is calculated by the ratio of  $M_w/M_n$ , which is generally to assess the molecular weight distribution. It can be seen that the polydispersity index was also declined as the addition content of PICPP increased. PLA was apt to decompose during the processing procedure because of the catalysis of hydroxyl terminated PICPP. That is why the decreased molecular weight and the increased polydispersity index after incorporating PICPP into PLA.

**Table 1:** GPC results of PLA and PLA/PICPP

	$M_n$ (Da)	$M_w$ (Da)	Polydispersity
PLA	686130	741408	1.08
PLA/PICPP-5	611919	697076	1.14
PLA/PICPP-10	537906	638488	1.19
PLA/PICPP-15	483370	591192	1.22

The effect of PICPP on the thermo-mechanical performances of PLA was determined using DMA measurement. Fig. 3a illustrates that the storage modulus ( $E'$ ) decreased with the increment of temperature in the whole studied scale. The  $E'$  at 30°C of the pristine PLA was 2,179 MPa, whereas the addition of PICPP decreased the  $E'$  at 30°C to 1,956, 1,716 and 1,551 MPa for PLA/PICPP-5, PLA/PICPP-10 and PLA/PICPP-15, respectively. The reduced storage modulus of the PLA/PICPP composites can be ascribed to the declined molecular weight of PLA catalyzed by the presence of PICPP. Additionally, all the samples exhibited a sharply decreased  $E'$  stage corresponding to the transition stage from the glassy state to the rubbery state of PLA. The glass transition temperature ( $T_g$ ) is identified by the temperature at the maximum  $\tan\delta$  value (Fig. 3b). The  $T_g$  of the pristine PLA was 73°C. When the addition content of PICPP was low, the  $T_g$  of PLA/PICPP-5 remained unchanged. With the increase of the addition content of PICPP, the  $T_g$  of PLA/PICPP-10 and PLA/PICPP-15 was slightly decreased to approximately 69°C. Moreover, the broaden long tail of  $\tan\delta$  peak could due to the fact that  $G''$  decreases slowly as temp increases, which implies the chain entanglements are enhanced, supporting the better compatibility.

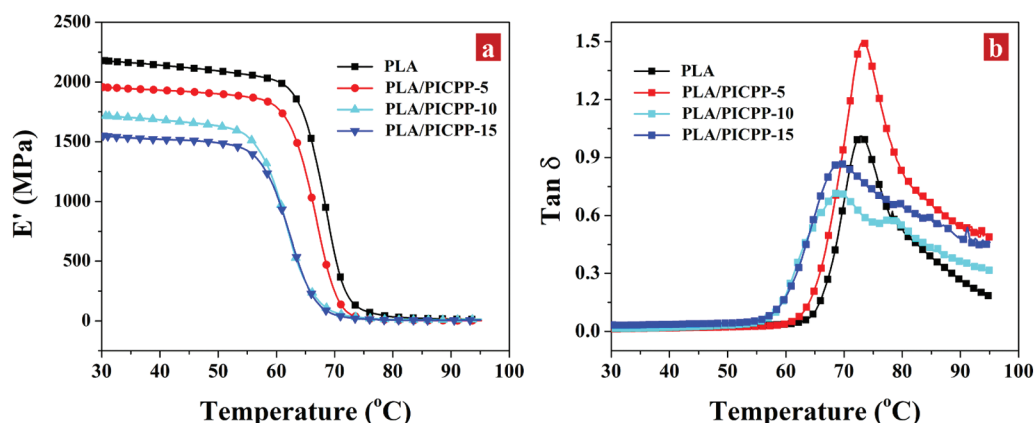


**Figure 3:** DMA plots of PLA and PLA/PICPP: (a) storage modulus ( $E'$ ) and (b)  $\tan \delta$

Typical stress-strain curves of PLA and its composites are shown in Fig. 4, corresponding data were summarized in Table 2. It can be observed that the incorporation of PICPP into PLA matrix showed a negative effect on the mechanical properties of PLA composites. The tensile modulus, tensile strength and elongation at break of pure PLA were 1.31 GPa, 66.45 MPa and 7.03%. Adding 5 wt% PICPP into PLA matrix, the tensile strength of PLA/PICPP-5 slightly declined to 59.79 MPa while the elongation at break of PLA/PICPP-5 increased to 7.81%, and PLA/PICPP-5 presented comparative tensile modulus as that of neat PLA. However, further increasing the addition of PICPP, the tensile strength and elongation at break of PLA/PICPP-10 and PLA/PICPP-15 were obviously decreased, which was attributed to that the presence of PICPP declined the molecular weight of PLA, hence worsening the mechanical properties of PLA composites.

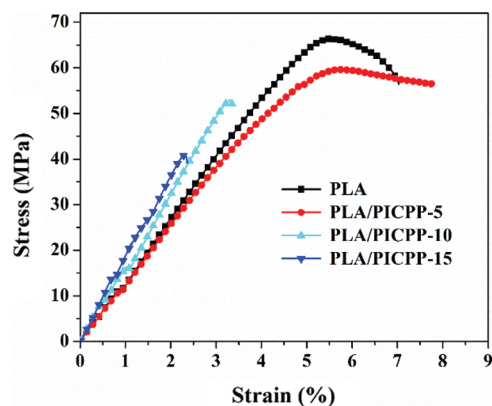


**Figure 4:** Typical stress-strain curves of PLA and its composites

**Table 2:** Tensile test data of PLA and its composites

Sample	Tensile modulus (GPa)	Tensile strength (MPa)	Elongation at break (%)
PLA	1.31	66.45	7.0
PLA/PICPP-5	1.30	59.79	7.8
PLA/PICPP-10	1.93	53.25	3.4
PLA/PICPP-15	2.00	41.31	2.4

The effect of PICPP on thermal decomposition of PLA was analyzed using TGA. Fig. 5 shows the TGA and differential TGA (DTG) thermograms of PLA and PLA/PICPP under air and nitrogen atmospheres, and Table 3 summarizes the relating data. In Figs. 5a and 5b, PLA thermally degraded in a single stage between 324°C ( $T_{5\%}$ , the temperature at 5% weight loss,) and 380°C, and the weight loss was 97.5%. The temperature at the maximum decomposition rate ( $T_m$ ) of PLA was 363°C as observed in the DTG curve. At 800°C, only 0.4% residue was left. After adding PICPP, PLA/PICPP thermally degraded in one stage. With the increase of the addition content of PICPP, the  $T_{5\%}$  of PLA/PICPP was decreased gradually, owing to the earlier decomposition of phosphorus-containing additives [48,49]. The presence of PICPP almost had no change in the residue yield of PLA. Although PICPP had certain charring ability, the formed char was unstable and decomposed at high temperature. Owing to the generation of the intermediate char, the weight loss rate was slowed down during the thermal decomposition process, as demonstrated by the DTG curves. Under nitrogen atmosphere, PLA also behaved a thermal decomposition stage between 333°C ( $T_{5\%}$ ) and 390°C and yield 1.0% residue (Figs. 5c and 5d). The  $T_{5\%}$  and  $T_m$  of PLA were slightly higher than those under air, because of the absence of oxidation by oxygen. Similarly, the  $T_{5\%}$  of PLA/PICPP was decreased gradually as the addition content of PICPP grew up. From DTG curves, it can be found that the incorporation of PICPP reduced the weight loss rate of PLA during the thermal decomposition process, which was ascribed to the generation of a carbonaceous layer. However, the char was thermally unstable so that cannot resist the high temperature. Thus, the residue yield of PLA/PICPP was very slightly improved by the presence of PICPP.

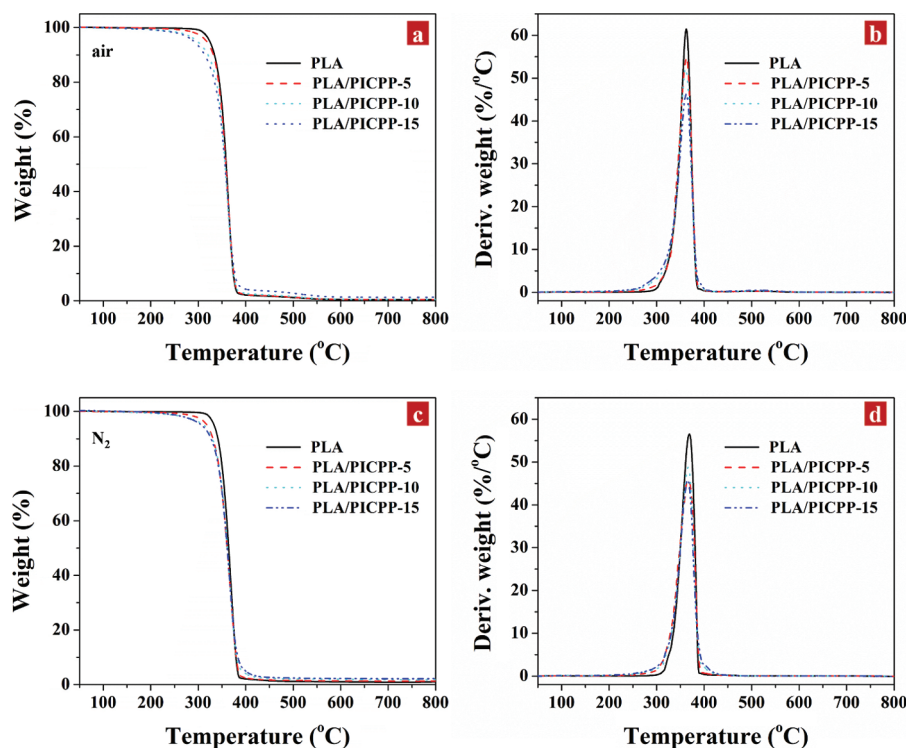


**Figure 5:** TGA and DTG thermograms of PLA and PLA/PICPP under (a, b) air and (c, d) nitrogen atmosphere

**Table 3:** Effect of PICPP content on the thermal decomposition of PLA under air and nitrogen atmosphere

	$T_{5\%}$ (°C)		$T_m$ (°C)		Residual yield (%) at 800 °C	
	Air	N <sub>2</sub>	Air	N <sub>2</sub>	Air	N <sub>2</sub>
PLA	324	333	363	369	0.4	1.0
PLA/PICPP-5	318	319	363	368	0.5	1.3
PLA/PICPP-10	298	312	361	367	0.5	1.8
PLA/PICPP-15	291	307	363	365	1.4	2.2

The LOI and UL-94 tests are employed to assess the anti-flammable behaviors of PLA and PLA/PICPP, and corresponding results are summarized in Table 4. The LOI value of pure PLA was 20.0% which was relatively low, and it completely burned out in the UL-94 test corresponding to no classification. With increasing the addition amount of PICPP, the LOI of PLA/PICPP composites was increased gradually. Specifically, the LOI value of PLA/PICPP-5, PLA/PICPP-10 and PLA/PICPP-15 was 26.0%, 30.0% and 31.0%, respectively. Additionally, PLA/PICPP-5 behaved UL-94 V-1 classification, and PLA/PICPP-10 and PLA/PICPP-15 achieved UL-94 V-0 classification, manifesting that PICPP was an efficient flame retardant additive for PLA. Since the dispersion behavior of flame retardants or the phase separation morphology has an impact on the flame retardant efficiency [50,51], such the high flame retardant effect could be ascribed to the good dispersion state of the PICPP in PLA matrix.

**Table 4:** LOI, UL-94 and MCC data of PLA and PLA/PICPP

	LOI (%)	UL-94	PHRR (W/g)	THR (kJ/g)	$T_p$ (°C)
PLA	20.0	Failed	690	24.6	371
PLA/PICPP-5	26.0	V-1	564	22.1	371
PLA/PICPP-10	30.0	V-0	537	21.9	369
PLA/PICPP-15	31.0	V-0	463	20.6	368

MCC is a widespread apparatus to obtain the heat release rate (HRR) information of polymers just using milligram samples [52,53]. Fig. 6 depicts the HRR vs. temperature curves of PLA and PLA/PICPP, and Table 4 summarizes the relating data. The HRR curve of the pristine PLA showed an intense peak, and its peak HRR (PHRR) value was 690 W/g, implying that PLA was a highly flammable material. With the content of PICPP was increased, the PHRR of PLA/PICPP was decreased gradually. Specifically, the PHRR values of PLA/PICPP-5, PLA/PICPP-10 and PLA/PICPP-15 were reduced to 564, 537 and 463 W/g, respectively. The PLA/PICPP-15 exhibited the lowest PHRR value, 33% lower than the pristine PLA. Additionally, the width of the HRR curves of PLA/PICPP composites became broaden with increasing the content of PICPP. This was consistent with the widen molecular weight distribution of PLA caused by the catalysis of PICPP. The THR value showed a similar changing trend as the PHRR. As increasing the content of PICPP, the THR values of PLA/PICPP-5, PLA/PICPP-10 and PLA/PICPP-15 were declined to 22.1, 21.9 and 20.6 kJ/g, respectively. By contrast to the pristine PLA, the temperature to PHRR ( $T_p$ ) of PLA/PICPP exhibited a quite slight change, whose changing trend was in good agreement with the  $T_{max}$  observed in DTG curves.

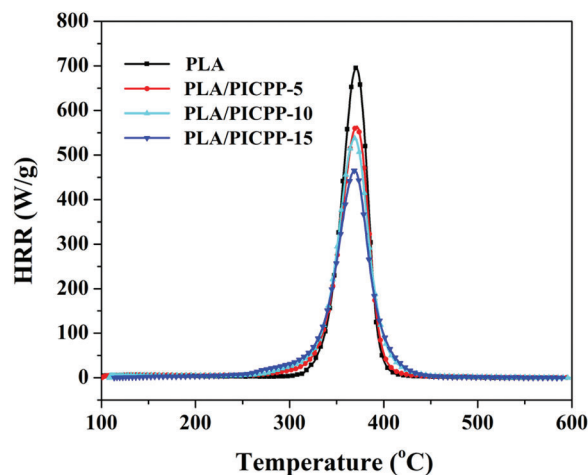


**Figure 6:** HRR vs. temperature plots of PLA and PLA/PICPP composites

The evolved products of PLA and PLA/PICPP-15 in the vapor phase were detected by TG-FTIR technique. As shown in Figs. 7a and 7b, it was apparent that PLA/PICPP-15 exhibited a similar 3D FTIR spectra as PLA. The typical evolved products appeared at 2,930–2,600, 1,870–1,650, 1,530–1,290, and 1,190–1,000  $\text{cm}^{-1}$  for both PLA and PLA/PICPP-15. Fig. 7c further provides the FTIR spectra of PLA and PLA/PICPP-15 at the maximum weight loss rate. The typical evolved products were identified by the characteristic signals: aliphatic hydrocarbons (stretching vibrations at 2,930–2,800  $\text{cm}^{-1}$ ; bending vibrations at 1,480–1,300  $\text{cm}^{-1}$ ), aldehydes (2,800–2,600  $\text{cm}^{-1}$ ), ketones and carboxylic acids (1,870–1,650  $\text{cm}^{-1}$ ) and esters (1,190–1,000  $\text{cm}^{-1}$ ) [11,23,54]. During the thermal decomposition process, the macromolecular chains of PLA broken into several typical small molecules including aliphatic hydrocarbons, aldehydes, ketones and carboxylic acids and esters, which accorded well with the previous reports [11,23]. Among these typical pyrolysis products, carbonyls (aldehydes, ketones and carboxylic acids, etc.) displayed the highest absorbance intensity, implying that they are the majority in the pyrolysis products. Additionally, the absorbance intensity of the peaks at 1,870–1,650  $\text{cm}^{-1}$  of PLA/PICPP-15 was lower than that of PLA, meaning the declined production of carbonyls in the decomposition process. Since carbonyls are flammable pyrolysis products, the declined carbonyl-moieties production may account for the declined heat release parameters in MCC measurement.

Based on the discussion above, the flame retardant mechanism of PICPP can be attributed to the combined gas and condensed phase flame retardant actions. The former plays a flame retardant effect by generating phosphorus-containing free radicals while the latter by forming pyrophosphoric acid or metaphosphoric acid compounds. According to the previous reports [55], the char yield decreased and the emission of phosphorus-containing volatiles increased as the oxidation state of phosphorus decreased. Because the PICPP has a low oxidation state of phosphorus, the flame retardant mode of action of PICPP mainly manifested in the gas phase. The gaseous phase flame retardant action is mainly depicted as follows: Once the PLA composites are exposed to fire sources, PICPP could decompose to generate phosphorus-containing free radicals, which can quench the hydrocarbon free radicals from the decomposed matrix and thus terminate the combustion chain reaction in gas phase. Additionally, some phosphorus-containing compounds derived from the thermal decomposition of PICPP remain in the condensed phase, resulting in the slight promotion of char yield as observed in TGA. Predominant gas phase mode of action in combination with minor carbonization has been reported to be an efficient strategy for flame retardancy enhancement [56].

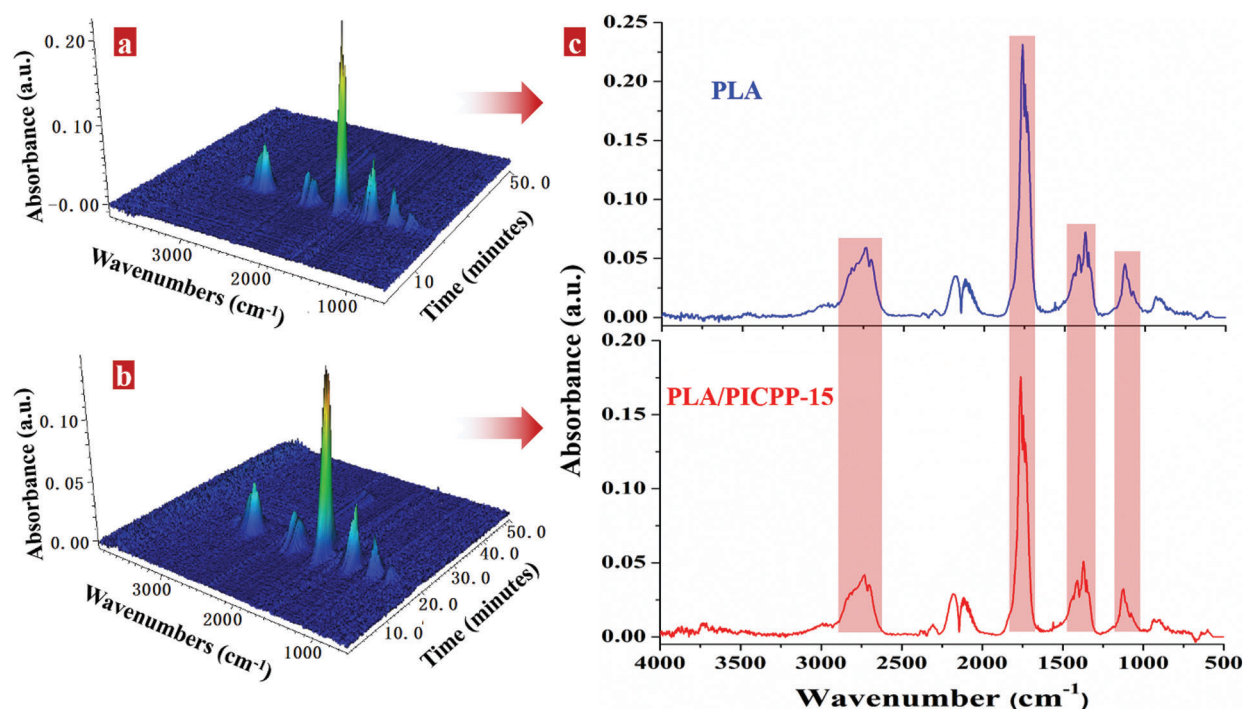


**Figure 7:** 3D FTIR spectra of the evolved products of (a) PLA and (b) PLA/PICPP-15; (c) FTIR spectra of the evolved products of PLA and PLA/PICPP-15 at the maximum decomposition rate

#### 4 Conclusions

In this study, an isosorbide-derived polyphosphonate (PICPP) was synthesized and utilized as an anti-flammable agent for PLA. FTIR and NMR spectral data demonstrated the successful synthesis of PICPP. Owing to the catalysis effect of hydroxyl-terminated PICPP on the decomposition of PLA during the processing, the molecular weight of PLA was declined after adding PICPP. The incorporation of PICPP led to a reduction in the storage modulus of PLA as the molecular weight was declined. TGA results manifested that PICPP reduced the onset thermal degradation temperature and the weight loss rate of PLA composites during the thermal decomposition process. PLA containing 10 wt% of PICPP achieved a high LOI value of 30.0% and passed the UL-94 V-0 classification. Additionally, the PHRR and THR of PLA containing 15 wt% of PICPP were declined by 33% and 16%, respectively, compared with those of PLA. TGA-FTIR results clarified that PLA/PICPP produced the less typical pyrolysis products especially flammable carbonyls than PLA, which was responsible for the declined PHRR and THR values of PLA/PICPP. This isosorbide-derived polyphosphonate provides a renewable and efficient solution for flame-retardant PLA.

**Funding Statement:** The work was financially supported by the Hong Kong Scholars Program (Grant No. XJ2020003) and the Basic Research Program of Jiangnan University (JUSRP121029).

**Conflicts of Interest:** The authors declare that they have no conflicts of interest to report regarding the present study.

#### References

1. Gross, R. A., Kalra, B. (2002). Biodegradable polymers for the environment. *Science*, 297(5582), 803–807. DOI 10.1126/science.297.5582.803.

2. Chow, W. S., Teoh, E. L., Karger-Kocsis, J. (2018). Flame retarded poly(lactic acid): A review. *Express Polymer Letters*, 12(5), 396–417. DOI 10.3144/expresspolymlett.2018.34.
3. Tawiah, B., Yu, B., Fei, B. (2018). Advances in flame retardant poly(lactic acid). *Polymers*, 10(8), 876. DOI 10.3390/Polym10080876.
4. Bourbigot, S., Fontaine, G. (2010). Flame retardancy of polylactide: An overview. *Polymer Chemistry*, 1(9), 1413–1422. DOI 10.1039/c0py00106f.
5. Yu, S., Hu, X., Tang, F., Zhu, C., Xiang, H. et al. (2020). Flame-retardant poly(lactic acid): An overview and outlook. *Chemical Industry and Engineering Progress*, 39(9), 3421–3432. DOI 10.16085/j.issn.1000-6613.2020-0320.
6. Wang, X., Sun, J., Liu, X., Jiang, S., Wang, J. et al. (2019). An effective flame retardant containing hypophosphorous acid for poly (lactic acid): Fire performance, thermal stability and mechanical properties. *Polymer Testing*, 78, 105940. DOI 10.1016/j.polymertesting.2019.105940.
7. Yemisci, F., Yesil, S., Aytac, A. (2017). Improvement of the flame retardancy of plasticized poly(lactic acid) by means of phosphorus-based flame retardant fillers. *Fire and Materials*, 41(8), 964–972. DOI 10.1002/fam.2440.
8. Jian, R. K., Xia, L., Ai, Y. F., Wang, D. Y. (2018). Novel dihydroxy-containing ammonium phosphate based poly (lactic acid): Synthesis, characterization and flame retardancy. *Polymers*, 10(8), 871. DOI 10.3390/Polym10080871.
9. Feng, J., Sun, Y., Song, P., Lei, W., Wu, Q. et al. (2017). Fire-resistant, strong, and green polymer nanocomposites based on poly(lactic acid) and core-shell nanofibrous flame retardants. *ACS Sustainable Chemistry & Engineering*, 5(9), 7894–7904. DOI 10.1021/acssuschemeng.7b01430.
10. Chen, Y. J., Wang, W., Liu, Z. Q., Yao, Y. Y., Qian, L. J. (2017). Synthesis of a novel flame retardant containing phosphazene and triazine groups and its enhanced charring effect in poly(lactic acid) resin. *Journal of Applied Polymer Science*, 134(13), 44660. DOI 10.1002/App.44660.
11. Wang, X., Hu, Y., Song, L., Xuan, S., Xing, W. et al. (2011). Flame retardancy and thermal degradation of intumescent flame retardant poly(lactic acid)/starch biocomposites. *Industrial & Engineering Chemistry Research*, 50(2), 713–720. DOI 10.1021/ie1017157.
12. Kang, B. H., Lu, X., Qu, J. P., Yuan, T. (2019). Synergistic effect of hollow glass beads and intumescent flame retardant on improving the fire safety of biodegradable poly (lactic acid). *Polymer Degradation and Stability*, 164, 167–176. DOI 10.1016/j.polymdegradstab.2019.04.013.
13. Zhao, X., Gao, S., Liu, G. S. (2016). A THEIC-based polyphosphate melamine intumescent flame retardant and its flame retardancy properties for polylactide. *Journal of Analytical and Applied Pyrolysis*, 122, 24–34. DOI 10.1016/j.jaap.2016.10.029.
14. Niu, M. J., Zhang, Z. Z., Wei, Z. Z., Wang, W. J. (2020). Effect of a novel flame retardant on the mechanical, thermal and combustion properties of poly(lactic acid). *Polymers*, 12(10), 2407. DOI 10.3390/polym12102407.
15. Gu, L. Q., Qiu, J. H., Sakai, E. (2017). Effect of DOPO-containing flame retardants on poly(lactic acid): Non-flammability, mechanical properties and thermal behaviors. *Chemical Research in Chinese Universities*, 33(1), 143–149. DOI 10.1007/s40242-017-6196-9.
16. Long, L., Chang, Q., He, W., Xiang, Y., Qin, S. et al. (2017). Effects of bridged DOPO derivatives on the thermal stability and flame retardant properties of poly(lactic acid). *Polymer Degradation and Stability*, 139, 55–66. DOI 10.1016/j.polymdegradstab.2017.03.016.
17. Zhang, T., Long, L. J., He, W. T., He, M., Qin, S. H. et al. (2019). Flame-retardant properties of 9, 10-dihydro-9-oxa-10-phosphaphenanthrene-10-oxide derivatives in poly(lactic acid). *Acta Polymerica Sinica*, 50(1), 71–81. DOI 10.11777/j.issn1000-3304.2018.18148.
18. Jia, L., Zhang, W. C., Tong, B., Yang, R. J. (2018). Crystallization, mechanical and flame-retardant properties of poly(lactic acid) composites with DOPO and DOPO-POSS. *Chinese Journal of Polymer Science*, 36(7), 871–879. DOI 10.1007/s10118-018-2098-7.
19. Wei, L. L., Wang, D. Y., Chen, H. B., Chen, L., Wang, X. L. et al. (2011). Effect of a phosphorus-containing flame retardant on the thermal properties and ease of ignition of poly(lactic acid). *Polymer Degradation and Stability*, 96(9), 1557–1561. DOI 10.1016/j.polymdegradstab.2011.05.018.

20. Lin, H. J., Han, L. J., Wang, X. M., Bian, Y. J., Li, Y. S. et al. (2013). Study on the thermal degradation behavior and flame-retardant property of polylactide/PEDPP blends. *Polymers for Advanced Technologies*, 24(6), 576–583. DOI 10.1002/pat.3120.
21. Lin, H. J., Liu, S. R., Han, L. J., Wang, X. M., Bian, Y. J. et al. (2013). Effect of a phosphorus-containing oligomer on flame-retardant, rheological and mechanical properties of poly(lactic acid). *Polymer Degradation and Stability*, 98(7), 1389–1396. DOI 10.1016/j.polymdegradstab.2013.03.025.
22. Sim, M. J., Cha, S. H. (2019). Efficient polymeric phosphorus flame retardant: Flame retardancy, thermal property, and physical property on polylactide. *Polymer Bulletin*, 76(7), 3463–3479. DOI 10.1007/s00289-018-2558-9.
23. Chen, X. L., Zhuo, J. L., Jiao, C. M. (2012). Thermal degradation characteristics of flame retardant polylactide using TG-IR. *Polymer Degradation and Stability*, 97(11), 2143–2147. DOI 10.1016/j.polymdegradstab.2012.08.016.
24. Wu, N. J., Fu, G. L., Yang, Y., Xia, M. F., Yun, H. et al. (2019). Fire safety enhancement of a highly efficient flame retardant poly(phenylphosphoryl phenylenediamine) in biodegradable poly(lactic acid). *Journal of Hazardous Materials*, 363, 1–9. DOI 10.1016/j.jhazmat.2018.08.090.
25. Yang, W., Tawiah, B., Yu, C., Qian, Y. F., Wang, L. L. et al. (2018). Manufacturing, mechanical and flame retardant properties of poly(lactic acid) biocomposites based on calcium magnesium phytate and carbon nanotubes. *Composites Part A: Applied Science and Manufacturing*, 110, 227–236. DOI 10.1016/j.compositesa.2018.04.027.
26. Wei, P., Bocchini, S., Camino, G. (2013). Flame retardant and thermal behavior of polylactide/expandable graphite composites. *Polimery*, 58(5), 361–364. DOI 10.14314/polimery.2013.361.
27. Tawiah, B., Yu, B., Yuen, R. K. K., Hu, Y., Wei, R. C. et al. (2019). Highly efficient flame retardant and smoke suppression mechanism of boron modified graphene oxide/poly(Lactic acid) nanocomposites. *Carbon*, 150, 8–20. DOI 10.1016/j.carbon.2019.05.002.
28. Yu, T., Jiang, N., Li, Y. (2014). Functionalized multi-walled carbon nanotube for improving the flame retardancy of ramie/poly(lactic acid) composite. *Composites Science and Technology*, 104, 26–33. DOI 10.1016/j.compscitech.2014.08.021.
29. Hou, Y. B., Liu, L. X., Qiu, S. L., Zhou, X., Gui, Z. et al. (2018). DOPO-Modified two-dimensional co-based metal-organic framework: Preparation and application for enhancing fire safety of poly(lactic acid). *ACS Applied Materials & Interfaces*, 10(9), 8274–8286. DOI 10.1021/acsami.7b19395.
30. Zhang, L., Chen, S. Q., Pan, Y. T., Zhang, S. D., Nie, S. B. et al. (2019). Nickel metal-organic framework derived hierarchically mesoporous nickel phosphate toward smoke suppression and mechanical enhancement of intumescent flame retardant wood fiber/poly(lactic acid) composites. *ACS Sustainable Chemistry & Engineering*, 7(10), 9272–9280. DOI 10.1021/acssuschemeng.9b00174.
31. Li, S. M., Yuan, H., Yu, T., Yuan, W. Z., Ren, J. (2009). Flame-retardancy and anti-dripping effects of intumescent flame retardant incorporating montmorillonite on poly(lactic acid). *Polymers for Advanced Technologies*, 20(12), 1114–1120. DOI 10.1002/pat.1372.
32. Chow, W. S., Teoh, E. L. (2015). Flexible and flame resistant poly(lactic acid)/organomontmorillonite nanocomposites. *Journal of Applied Polymer Science*, 132(2), 41253. DOI 10.1002/App.41253.
33. Suparanon, T., Surisaeng, J., Phusunti, N., Phetwarotai, W. (2018). Synergistic efficiency of tricresyl phosphate and montmorillonite on the mechanical characteristics and flame retardant properties of polylactide and poly(butylene succinate) blends. *Chinese Journal of Polymer Science*, 36(5), 620–631. DOI 10.1007/s10118-018-2043-9.
34. Tang, G., Deng, D., Chen, J., Zhou, K. Q., Zhang, H. et al. (2017). The influence of organo-modified sepiolite on the flame-retardant and thermal properties of intumescent flame-retardant polylactide composites. *Journal of Thermal Analysis and Calorimetry*, 130(2), 763–772. DOI 10.1007/s10973-017-6425-y.
35. Zhou, Y., Huang, J., Wang, J., Chu, F., Xu, Z. et al. (2020). Rationally designed functionalized black phosphorus nanosheets as new fire hazard suppression material for polylactic acid. *Polymer Degradation and Stability*, 178, 109194. DOI 10.1016/j.polymdegradstab.2020.109194.
36. Cao, X. W., Chi, X. N., Deng, X. Q., Liu, T., Yu, B. et al. (2020). Synergistic effect of flame retardants and graphitic carbon nitride on flame retardancy of polylactide composites. *Polymers for Advanced Technologies*, 31(7), 1661–1670. DOI 10.1002/pat.4894.

37. Xu, L. F., Tan, X. W., Xu, R. J., Xie, J. Y., Lei, C. H. (2019). Influence of functionalized molybdenum disulfide (MoS<sub>2</sub>) with triazine derivatives on the thermal stability and flame retardancy of intumescent poly(lactic acid) system. *Polymer Composites*, 40(6), 2244–2257. DOI 10.1002/pc.25032.
38. Gao, R., Wang, S. G., Zhou, K. Q., Qian, X. D. (2019). Mussel-inspired decoration of Ni(OH)<sub>2</sub> nanosheets on 2D MoS<sub>2</sub> towards enhancing thermal and flame retardancy properties of poly(lactic acid). *Polymers for Advanced Technologies*, 30(4), 879–888. DOI 10.1002/pat.4521.
39. Zhang, S., Jin, X. D., Gu, X. Y., Chen, C., Li, H. F. et al. (2018). The preparation of fully bio-based flame retardant poly(lactic acid) composites containing casein. *Journal of Applied Polymer Science*, 135(33), 46599. DOI 10.1002/App.46599.
40. Costes, L., Laoutid, F., Dumazert, L., Lopez-cuesta, J. M., Brohez, S. et al. (2015). Metallic phytates as efficient bio-based phosphorous flame retardant additives for poly(lactic acid). *Polymer Degradation and Stability*, 119, 217–227. DOI 10.1016/j.polymdegradstab.2015.05.014.
41. Vahabi, H., Shabanian, M., Aryanasab, F., Mangin, R., Laoud, F. et al. (2018). Inclusion of modified lignocellulose and nano-hydroxyapatite in development of new bio-based adjuvant flame retardant for poly(lactic acid). *Thermochimica Acta*, 666, 51–59. DOI 10.1016/j.tca.2018.06.004.
42. Jin, X. B., Xiang, E., Zhang, R., Qin, D. C., Jiang, M. L. et al. (2021). Halloysite nanotubes immobilized by chitosan/tannic acid complex as a green flame retardant for bamboo fiber/poly(lactic acid) composites. *Journal of Applied Polymer Science*, 138(1), 49621. DOI 10.1002/app.49621.
43. Łukaszczyk, J., Janicki, B., Kaczmarek, M. (2011). Synthesis and properties of isosorbide based epoxy resin. *European Polymer Journal*, 47(8), 1601–1606. DOI 10.1016/j.eurpolymj.2011.05.009.
44. Daniel, Y. G., Howell, B. A. (2018). Phosphorus flame retardants from isosorbide bis-acrylate. *Polymer Degradation and Stability*, 156, 14–21. DOI 10.1016/j.polymdegradstab.2018.07.027.
45. Daniel, Y. G., Howell, B. A. (2017). Flame retardant properties of isosorbide bis-phosphorus esters. *Polymer Degradation and Stability*, 140, 25–31. DOI 10.1016/j.polymdegradstab.2017.04.005.
46. Hu, C., Bourbigot, S., Delaunay, T., Collinet, M., Marcille, S. et al. (2019). Synthesis of isosorbide based flame retardants: Application for polybutylene succinate. *Polymer Degradation and Stability*, 164, 9–17. DOI 10.1016/j.polymdegradstab.2019.03.016.
47. Wang, X., Niu, H. X., Guo, W. W., Song, L., Hu, Y. (2021). Renewable isosorbide-derived poly(phosphoester) for simultaneously enhanced flame-retardancy and mechanical property of polylactide. *Progress in Natural Science: Materials International*, 31(4), 546–556. DOI 10.1016/j.pnsc.2021.06.004.
48. Wang, X., Hu, Y., Song, L., Xing, W., Lu, H. D. et al. (2010). Flame retardancy and thermal degradation mechanism of epoxy resin composites based on a DOPO substituted organophosphorus oligomer. *Polymer*, 51(11), 2435–2445. DOI 10.1016/j.polymer.2010.03.053.
49. Wang, X., Song, L., Xing, W. Y., Lu, H. D., Hu, Y. (2011). A effective flame retardant for epoxy resins based on poly(DOPO substituted dihydroxyl phenyl pentaerythritol diphosphonate). *Materials Chemistry and Physics*, 125(3), 536–541. DOI 10.1016/j.matchemphys.2010.10.020.
50. Guo, Y. C., Xue, Y., Zuo, X., Zhang, L., Yang, Z. et al. (2017). Capitalizing on the molybdenum disulfide/graphene synergy to produce mechanical enhanced flame retardant ethylene-vinyl acetate composites with low aluminum hydroxide loading. *Polymer Degradation and Stability*, 144, 155–166. DOI 10.1016/j.polymdegradstab.2017.08.015.
51. Xue, Y., Zuo, X., Wang, L., Zhou, Y., Pan, Y. et al. (2020). Enhanced flame retardancy of poly(lactic acid) with ultra-low loading of ammonium polyphosphate. *Composites Part B: Engineering*, 196, 108124. DOI 10.1016/j.compositesb.2020.108124.
52. Guo, W. W., Yu, B., Yuan, Y., Song, L., Hu, Y. (2017). In situ preparation of reduced graphene oxide/DOPO-based phosphonamidate hybrids towards high-performance epoxy nanocomposites. *Composites Part B: Engineering*, 123, 154–164. DOI 10.1016/j.compositesb.2017.05.024.
53. Wang, F., Zhang, P., Mou, Y., Kang, M., Liu, M. et al. (2017). Synthesis of the polyethylene glycol solid-solid phase change materials with a functionalized graphene oxide for thermal energy storage. *Polymer Testing*, 63, 494–504. DOI 10.1016/j.polymertesting.2017.09.005.

54. Guo, W. W., Wang, X., Gangireddy, C. S. R., Wang, J., Pan, Y. et al. (2019). Cardanol derived benzoxazine in combination with boron-doped graphene toward simultaneously improved toughening and flame retardant epoxy composites. *Composites Part A: Applied Science and Manufacturing*, 116, 13–23. DOI 10.1016/j.compositesa.2018.10.010.
55. Braun, U., Balabanovich, A. I., Scharrel, B., Knoll, U., Artner, J. et al. (2006). Influence of the oxidation state of phosphorus on the decomposition and fire behaviour of flame-retarded epoxy resin composites. *Polymer*, 47(26), 8495–8508. DOI 10.1016/j.polymer.2006.10.022.
56. Perret, B., Scharrel, B., Stoss, K., Ciesielski, M., Diederichs, J. et al. (2011). A new halogen-free flame retardant based on 9, 10-dihydro-9-oxa-10-phosphaphenanthrene-10-oxide for epoxy resins and their carbon fiber composites for the automotive and aviation industries. *Macromolecular Materials and Engineering*, 296(1), 14–30. DOI 10.1002/mame.201000242.